

An Integrating Velocity–Azimuth Process Single-Doppler Radar Wind Retrieval Method

XUDONG LIANG

Laboratory of Typhoon Forecast Technique, Shanghai Typhoon Institute, China Meteorological Administration, Shanghai, China

(Manuscript received 26 June 2006, in final form 29 August 2006)

ABSTRACT

Among the single-Doppler radar wind analysis methods, the velocity–azimuth display (VAD), velocity–azimuth process (VAP), and uniform-wind (UW) methods are widely used because of their simplicity. This paper shows that the VAD, VAP, and UW methods can all be derived from the same relationship based on the azimuthal uniform-wind assumption. Using this assumption, an integrating VAP (IVAP) method is developed that can provide a smoother wind field than the VAP and UW methods and a higher resolution than the VAD method. Using the IVAP technique, the wind fields associated with a heavy rainfall case in Shanghai, China, are retrieved and compared with those from surface observations and wind-profiler data.

1. Introduction

Single-Doppler radar observations only give one component of the velocity field. To retrieve the entire velocity field, assumptions have to be made on either the spatial or temporal dependence of the velocity fields. The Tracking Radar Echo by Correlation (TREC) method was developed to estimate the velocity field from motion of the echoes (Zawadzki 1973; Rinehart 1979; Tuttle and Foote 1990). This method is based on the assumption that the radar echoes (or Doppler velocity patterns) are only moved by winds and there is no growth or decay. However, the TREC method does not take into account the velocity information directly. Recently, some more sophisticated wind retrieval methods that use prognostic equations or numerical models as strong or weak constraints in a variational framework have been developed (e.g., Sun et al. 1991; Kapitza 1991; Qiu and Xu 1992; Xu et al. 1994a,b, 1995; Shapiro et al. 2003). Although using complicated constraints may give a better estimate of the wind field, these methods are difficult to implement due to their complication and high computation cost.

On the other hand, some widely used methods have relative conceptual and practical simplicity. Among them, the simplest one is the velocity–azimuth display (VAD) technique, which is based on the assumption that the wind field varies linearly in space (Browning and Wexler 1968; Waldteufel and Corbin 1979; Caya and Zawadzki 1992). The uniform-wind (UW) method was developed by Persson and Andersson (1987) under the assumption that wind field is uniform in a limited region. The same assumption is also used in the velocity–azimuth process (VAP; Tao 1992) method.

The advantage of VAD is that it is not affected by small turbulence of the radial wind along the azimuth, to which UW and VAP methods are very sensitive. Nevertheless, the VAD method has a very poor spatial resolution compared with the UW and VAP methods. In this paper, it will be shown that the VAD, VAP, and UW methods can be combined to retrieve the wind field with a required resolution or smoothness.

The relationships among the VAD, VAP, and UW method are derived in section 2. A new integrating VAP (IVAP) method is then developed in section 3 and its characteristics are analyzed by using its frequency response function. Application of the IVAP method in a case study is presented in section 4, followed by conclusions and discussion in section 5.

Corresponding author address: Xudong Liang, Shanghai Typhoon Institute, 166 Puxi Road, Shanghai, 200030, China.
E-mail: liangxd@mail.typhoon.gov.cn

2. Relationship among the VAD, VAP, and UW methods

With a low-elevation scan, the effects of fall velocity and elevation angle may be neglected. The value of the radial velocity V_β (positive away from the radar) observed at fixed range and elevation can be expressed as

$$V_\beta = u_\beta \sin\beta + v_\beta \cos\beta, \tag{2.1}$$

where β is the azimuth angle measured from north, and u_β and v_β the Cartesian velocity u and v measured in radar coordinates (r, β) . Multiplying $\sin\beta$ or $\cos\beta$ on the both sides of (2.1) and integrating within the azimuth angle sector $[\beta_1, \beta_2]$ gives

$$\int_{\beta_1}^{\beta_2} V_\beta \sin\beta \, d\beta = \int_{\beta_1}^{\beta_2} u_\beta \sin^2\beta \, d\beta + \int_{\beta_1}^{\beta_2} v_\beta \cos\beta \sin\beta \, d\beta \tag{2.2a}$$

and

$$\bar{u} = \frac{\int_{\beta_1}^{\beta_2} V_\beta \cos\beta \, d\beta \int_{\beta_1}^{\beta_2} \sin^2\beta \, d\beta - \int_{\beta_1}^{\beta_2} V_\beta \sin\beta \, d\beta \int_{\beta_1}^{\beta_2} \cos\beta \sin\beta \, d\beta}{\int_{\beta_1}^{\beta_2} \sin^2\beta \, d\beta \int_{\beta_1}^{\beta_2} \cos^2\beta \, d\beta - \left(\int_{\beta_1}^{\beta_2} \cos\beta \sin\beta \, d\beta \right)^2} \tag{2.4a}$$

and

$$\bar{v} = \frac{\int_{\beta_1}^{\beta_2} V_\beta \sin\beta \, d\beta \int_{\beta_1}^{\beta_2} \cos^2\beta \, d\beta - \int_{\beta_1}^{\beta_2} V_\beta \cos\beta \, d\beta \int_{\beta_1}^{\beta_2} \sin\beta \cos\beta \, d\beta}{\int_{\beta_1}^{\beta_2} \cos^2\beta \, d\beta \int_{\beta_1}^{\beta_2} \sin^2\beta \, d\beta - \left(\int_{\beta_1}^{\beta_2} \sin\beta \cos\beta \, d\beta \right)^2} \tag{2.4b}$$

Equations (2.4a) and (2.4b) give the general approach to retrieve wind fields based on the azimuth uniform-wind assumption. The most important property of (2.4a) and (2.4b) is that the sector $[\beta_1, \beta_2]$ is not fixed and the uniform-wind assumption is only required within the given sector. If the sector $[\beta_1, \beta_2]$ is as large as one period (i.e., $[0, 2\pi]$), (2.4a) and (2.4b) reduce to

$$\bar{u} = \frac{\int_0^{2\pi} V_\beta \cos\beta \, d\beta}{\int_0^{2\pi} \cos^2\beta \, d\beta} \tag{2.5a}$$

and

$$\bar{v} = \frac{\int_0^{2\pi} V_\beta \sin\beta \, d\beta}{\int_0^{2\pi} \sin^2\beta \, d\beta} \tag{2.5b}$$

$$\int_{\beta_1}^{\beta_2} V_\beta \cos\beta \, d\beta = \int_{\beta_1}^{\beta_2} u_\beta \sin\beta \cos\beta \, d\beta + \int_{\beta_1}^{\beta_2} v_\beta \cos^2\beta \, d\beta. \tag{2.2b}$$

If the wind field is assumed to be uniform and independent of β within $[\beta_1, \beta_2]$, (2.2a) and (2.2b) can be expressed as

$$\int_{\beta_1}^{\beta_2} V_\beta \sin\beta \, d\beta = \bar{u} \int_{\beta_1}^{\beta_2} \sin^2\beta \, d\beta + \bar{v} \int_{\beta_1}^{\beta_2} \cos\beta \sin\beta \, d\beta \tag{2.3a}$$

and

$$\int_{\beta_1}^{\beta_2} V_\beta \cos\beta \, d\beta = \bar{u} \int_{\beta_1}^{\beta_2} \sin\beta \cos\beta \, d\beta + \bar{v} \int_{\beta_1}^{\beta_2} \cos^2\beta \, d\beta, \tag{2.3b}$$

where \bar{u} and \bar{v} are the uniform wind (mean flow) in sector $[\beta_1, \beta_2]$. Combining (2.3a) and (2.3b) gives

because $\int_0^{2\pi} \cos\beta \sin\beta \, d\beta = 0$. Equations (2.5a) and (2.5b) are used in the VAD method to retrieve mean wind fields within a given range. With a large sector, (2.4a) and (2.4b) can be used to retrieve a smooth wind field with a low horizontal resolution. Practically, the integrands in (2.4a) and (2.4b) are replaced by a sum. For a smaller sector $[\beta', \beta_2]$ (e.g., less than 10°) and only considering the two endpoints β_1 and β_2 , (2.4a) and (2.4b) change to

$$\int_{\beta_1}^{\beta_2} V_\beta \cos\beta \, d\beta \cong \sum_{\beta=\beta_1}^{\beta_2} V_\beta \cos\beta = V_{\beta_1} \cos\beta_1 + V_{\beta_2} \cos\beta_2,$$

so that (2.4a) and (2.4b) become

$$\bar{u} = \frac{V_{\beta_2} \sin\beta_1 - V_{\beta_1} \sin\beta_2}{\sin\beta_1 \cos\beta_2 - \sin\beta_2 \cos\beta_1} = \frac{V_{\beta_2} \sin\beta_1 - V_{\beta_1} \sin\beta_2}{\sin\Delta\beta}, \tag{2.6a}$$

and

$$\bar{v} = \frac{V_{\beta_2} \cos\beta_1 - V_{\beta_1} \cos\beta_2}{\sin\beta_1 \cos\beta_2 - \sin\beta_2 \cos\beta_1} = \frac{V_{\beta_2} \cos\beta_1 - V_{\beta_1} \cos\beta_2}{\sin\Delta\beta}, \quad (2.6b)$$

where $\Delta\beta = \beta_2 - \beta_1$. Equations (2.6a) and (2.6b) are the relationships used to retrieve the wind field in the

VAP method. A higher horizontal resolution can be achieved than using the VAD method because the uniform-wind assumption is only required in a small azimuth sector.

When $\Delta\beta \rightarrow 0$,

$$\sin\Delta\beta \rightarrow \Delta\beta \quad \text{and} \quad \cos\Delta\beta \rightarrow 1$$

so that (2.6a) becomes

$$\bar{u} = \frac{V_{\beta_2} \sin\beta_1 - V_{\beta_1} (\sin\beta_1 \cos\Delta\beta - \cos\beta_1 \sin\Delta\beta)}{\sin\Delta\beta} = V_{\beta_1} \cos\beta_1 + \frac{(V_{\beta_2} - V_{\beta_1}) \sin\beta_1 \Delta\beta \rightarrow 0}{\Delta\beta} = V_{\beta} \cos\beta + \frac{\partial V_{\beta}}{\partial \beta} \sin\beta, \quad (2.7a)$$

and similarly (2.6b) reduces to

$$\bar{v} = -V_{\beta} \sin\beta + \frac{\partial V_{\beta}}{\partial \beta} \cos\beta. \quad (2.7b)$$

Equations (2.7a) and (2.7b) are used in the UW method to retrieve the wind field with a higher horizontal resolution.

These derivations therefore demonstrate that the relationships used to retrieve the wind fields in the VAD, VAP, and UW methods are all special cases of the retrieval function based on the azimuthal uniform-wind assumption shown in (2.4a) and (2.4b) for a given azimuth sector $[\beta_1, \beta_2]$.

3. Integrating VAP method

In this section, the more general case represented in (2.4a) and (2.4b) is examined further. When using (2.4a) and (2.4b), the length of sector $[\beta_1, \beta_2]$ can be

changed according to the requirement of smoothness or resolution. The larger (smaller) the sector length is, the coarser (finer) horizontal resolution the wind field is and the more insensitive (sensitive) it is to small-scale turbulence. Because the information inside sector $[\beta_1, \beta_2]$ is used to retrieve the wind fields instead of only the information at the two ends β_1 and β_2 , the method using (2.4a) and (2.4b) to retrieve wind fields will be referred to as the IVAP method.

If the radar-observed radial winds are regarded as a combination of a set of waves with different frequencies, the wind retrieval method can be considered as a filter. Passing through this filter, some waves in the original signal are filtered out while the others are kept. This property can be examined using the frequency response function.

To obtain the frequency response function of the IVAP, we first substitute (2.1) into the right side of (2.4a) to obtain

$$\frac{\int_{\beta_1}^{\beta_2} (u_{\beta} \cos\beta + v_{\beta} \sin\beta) \cos\beta \, d\beta \int_{\beta_1}^{\beta_2} \sin^2\beta \, d\beta - \int_{\beta_1}^{\beta_2} (u_{\beta} \cos\beta + v_{\beta} \sin\beta) \sin\beta \, d\beta \int_{\beta_1}^{\beta_2} \cos\beta \sin\beta \, d\beta}{\int_{\beta_1}^{\beta_2} \sin^2\beta \, d\beta \int_{\beta_1}^{\beta_2} \cos^2\beta \, d\beta - \left(\int_{\beta_1}^{\beta_2} \cos\beta \sin\beta \, d\beta \right)^2} = \frac{\left(\int_{\beta_1}^{\beta_2} u_{\beta} \cos^2\beta \, d\beta + \frac{1}{2} \int_{\beta_1}^{\beta_2} v_{\beta} \, d \sin^2\beta \right) \int_{\beta_1}^{\beta_2} \sin^2\beta \, d\beta - \int_{\beta_1}^{\beta_2} u_{\beta} \cos\beta \sin\beta \, d\beta \int_{\beta_1}^{\beta_2} \cos\beta \sin\beta \, d\beta - \frac{1}{2} \int_{\beta_1}^{\beta_2} v_{\beta} \sin^2\beta \, d\beta \int_{\beta_1}^{\beta_2} d \sin^2\beta}{\int_{\beta_1}^{\beta_2} \sin^2\beta \, d\beta \int_{\beta_1}^{\beta_2} \cos^2\beta \, d\beta - \left(\int_{\beta_1}^{\beta_2} \cos\beta \sin\beta \, d\beta \right)^2}. \quad (3.1)$$

Omitting the difference between $\frac{1}{2} \int_{\beta_1}^{\beta_2} v_{\beta} \sin^2\beta \, d\beta \int_{\beta_1}^{\beta_2} d \sin^2\beta$ and $\frac{1}{2} \int_{\beta_1}^{\beta_2} v_{\beta} \, d \sin^2\beta \int_{\beta_1}^{\beta_2} \sin^2\beta \, d\beta$, (3.1) changes to

$$\frac{\int_{\beta_1}^{\beta_2} u_\beta \cos^2 \beta \, d\beta \int_{\beta_1}^{\beta_2} \sin^2 \beta \, d\beta - \int_{\beta_1}^{\beta_2} u_\beta \cos \beta \sin \beta \, d\beta \int_{\beta_1}^{\beta_2} \cos \beta \sin \beta \, d\beta}{\int_{\beta_1}^{\beta_2} \sin^2 \beta \, d\beta \int_{\beta_1}^{\beta_2} \cos^2 \beta \, d\beta - \left(\int_{\beta_1}^{\beta_2} \cos \beta \sin \beta \, d\beta \right)^2} \tag{3.2}$$

Assuming u_β has a waveform of

$$u_\beta = A \cos k\beta, \tag{3.3}$$

where A is the amplitude and k the wavenumber, (3.2) is rewritten as

$$\frac{\int_{\beta_1}^{\beta_2} A \cos k\beta \cos^2 \beta \, d\beta \int_{\beta_1}^{\beta_2} \sin^2 \beta \, d\beta - \int_{\beta_1}^{\beta_2} A \cos k\beta \cos \beta \sin \beta \, d\beta \int_{\beta_1}^{\beta_2} \cos \beta \sin \beta \, d\beta}{\int_{\beta_1}^{\beta_2} \sin^2 \beta \, d\beta \int_{\beta_1}^{\beta_2} \cos^2 \beta \, d\beta - \left(\int_{\beta_1}^{\beta_2} \cos \beta \sin \beta \, d\beta \right)^2} = A \frac{\int_{\beta_1}^{\beta_2} \cos k\beta \cos^2 \beta \, d\beta \int_{\beta_1}^{\beta_2} \sin^2 \beta \, d\beta - \int_{\beta_1}^{\beta_2} \cos k\beta \cos \beta \sin \beta \, d\beta \int_{\beta_1}^{\beta_2} \cos \beta \sin \beta \, d\beta}{\int_{\beta_1}^{\beta_2} \sin^2 \beta \, d\beta \int_{\beta_1}^{\beta_2} \cos^2 \beta \, d\beta - \left(\int_{\beta_1}^{\beta_2} \cos \beta \sin \beta \, d\beta \right)^2} \tag{3.4}$$

In the right-hand side of (3.4) the A is the original amplitude of a given wave, and the residual term gives a ratio of the output and input amplitude of a wave with the angular frequency of $k/2\pi$, which is the frequency response function of IVAP.

Because $\cos\beta$ and $\sin\beta$ are orthogonal, $\int_{\beta_1}^{\beta_2} \sin^2 \beta d\beta \int_{\beta_1}^{\beta_2} \cos^2 \beta d\beta \gg (\int_{\beta_1}^{\beta_2} \cos \beta \sin \beta d\beta)^2$ when $\beta_1 \neq \beta_2 \neq 0$; the frequency response function (3.4) is further reduced to

$$\frac{\int_{\beta_1}^{\beta_2} \cos k\beta \cos^2 \beta \, d\beta}{\int_{\beta_1}^{\beta_2} \cos^2 \beta \, d\beta} \tag{3.5}$$

If (3.5) is less (greater) than 1, the amplitude of the wave is reduced (magnified) by the filter.

Equation (3.5) suggests that, in general, the IVAP method can filter small-scale waves with a larger sector length of $[\beta_1, \beta_2]$ because $\int_{\beta_1}^{\beta_2} \cos^2 \beta d\beta$ is greater than $\int_{\beta_1}^{\beta_2} \cos k\beta \cos^2 \beta d\beta$ with a larger sector length [i.e., (3.5) is less than 1]. On the other hand, the larger the wavenumber k is (i.e., shorter wave), the smaller the value of $\int_{\beta_1}^{\beta_2} \cos k\beta \cos^2 \beta d\beta$ is [i.e., the smaller (3.5) is]. Hence the IVAP method can filter out small-scale waves.

Therefore, the IVAP method can produce a wind field with a coarse horizontal resolution or a wind field with a finer horizontal resolution by adjusting the length of the sector $[\beta_1, \beta_2]$. The larger the sector length is, the more precise is the wind. Because of the short-

wave filter property of the IVAP, the shortwave filter (e.g., smoothing operator) required in the VAP or UW method is not necessary.

The shortwave filter property of the IVAP method can be shown by an ideal experiment. Assume a radar observation of uniform flow $u = 10 \text{ m s}^{-1}$, $v = 0$. Both VAP and IVAP can retrieve the wind field exactly. When there is a random disturbance with a maximum amplitude of 0.5 m s^{-1} in the radar observation, the VAP and IVAP methods give different results (Fig. 1) with a different sector length (i.e., 6° , 12° , 24° , and 48°).

The retrieved wind u along the azimuth of 90° is shown in Fig. 1. Because the VAP method is sensitive to the small disturbance, the retrieved winds (Fig. 1a) have larger errors in all of the results with different sector length. However, the retrieved wind has smaller error when the sector length is larger (e.g., 48°) in the IVAP method retrieved winds (Fig. 1b) because of the shortwave filter property of the IVAP method, which also can be shown by average wind and square mean error of retrieved wind fields (Table 1). The square mean error of the VAP method is about 0.2 in all results with different sector length, but reduces to 0.072 in the IVAP method when using a sector length of 48° .

4. Case study

Using the IVAP method, the low-level wind field of a heavy rainfall case that occurred in Shanghai, China, on 5 August 2001 is retrieved using Doppler winds with

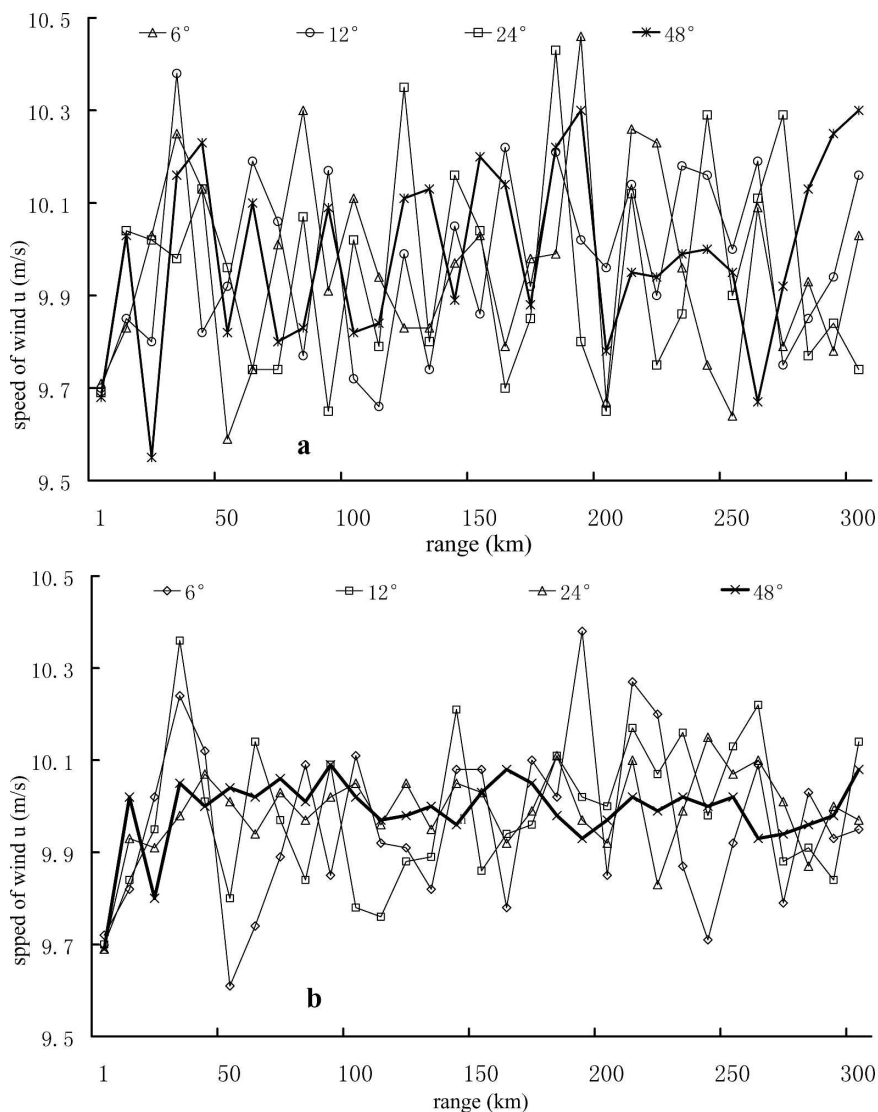


FIG. 1. The (a) VAP- and (b) IVAP-retrieved wind u along the azimuth 90° using radar-observed winds with random disturbance.

an elevation of 1° . On this day, heavy rainfall caused by a landfalling tropical cyclone produced a record of over 200 mm in 12 h (Fu et al. 2004). The radial winds of the Doppler radar Gemtronic 360AC located at Hongqiao Airport are used to retrieve the low-level wind fields.

Because varying the length of the sector $[\beta_1, \beta_2]$ can produce different results with different properties, the wind fields at 0900 UTC 5 August are retrieved using sector lengths of 9° , 18° , 45° and 90° , respectively (Fig. 2). As shown in Fig. 2, with smaller length, more details of wind fields are revealed such as the cyclonic flow in the northwestern sector in Figs. 2a and 2b, which can be inferred from surface observations (Fig. 2e). When the length is larger, the retrieved wind fields are smoother, such as in Figs. 2c and 2d.

To examine the retrieved winds in further detail observations from a wind-profiler located at Qingpu of Shanghai, northwest of the radar station, are used. The radar beam is about 550-m altitude at Qingpu when the elevation angle is 1° . The wind-profiler data averaged between altitude 520 and 570 m are therefore used to compare with retrieved wind. The wind-profiler and

TABLE 1. The average/square mean error of retrieved wind fields.

Sector length	6°	12°	24°	48°
IVAP	9.998/0.161	10.000/0.128	9.999/0.091	9.997/0.072
VAP	9.982/0.209	10.008/0.191	10.002/0.199	9.997/0.188

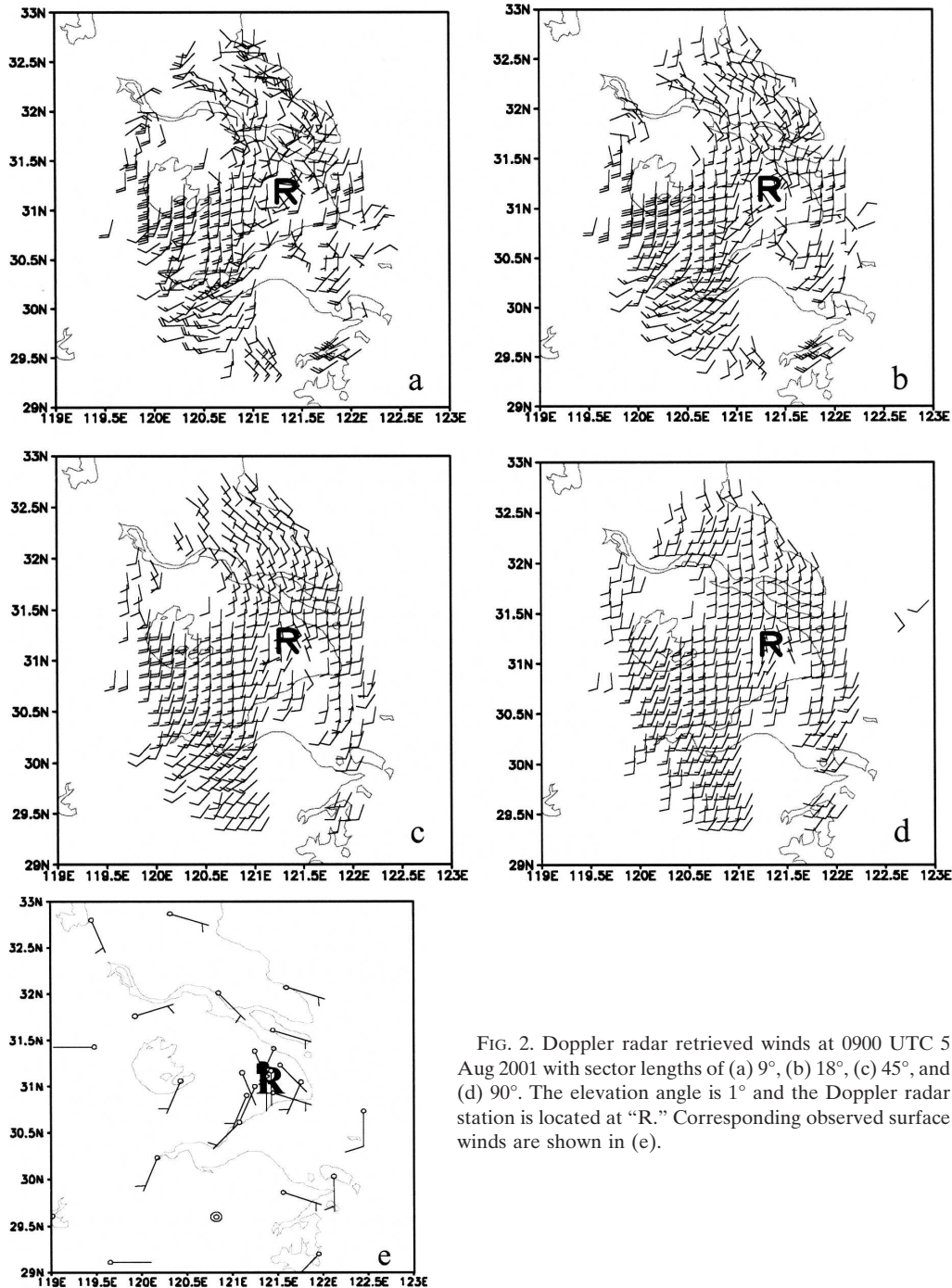


FIG. 2. Doppler radar retrieved winds at 0900 UTC 5 Aug 2001 with sector lengths of (a) 9° , (b) 18° , (c) 45° , and (d) 90° . The elevation angle is 1° and the Doppler radar station is located at "R." Corresponding observed surface winds are shown in (e).

radar data within 20-min time difference are taken as concomitant observations. From 0735 to 2035 UTC 5 August, there are 20 sets of valid observations.

The radar-retrieved winds are close to the wind-profiler observations (Fig. 3), and a larger sector length gives a smoother retrieved wind. The rapid increase of u near 1300 UTC (Fig. 3a) is also captured by the radar-retrieved winds. The correlation coefficients of wind-

profiler observed and radar-retrieved u (Table 2) are about 0.85 and the square mean errors reduced from 2.29 to 2.04 when the retrieval sector length changed from 9° to 90° . The correlation coefficients of v are increased from 0.401 to 0.625 and the square mean errors reduced from 3.61 to 2.30. It is shown that when the retrieval sector length is larger, the retrieval wind is more accurate. However, when using a sector length of

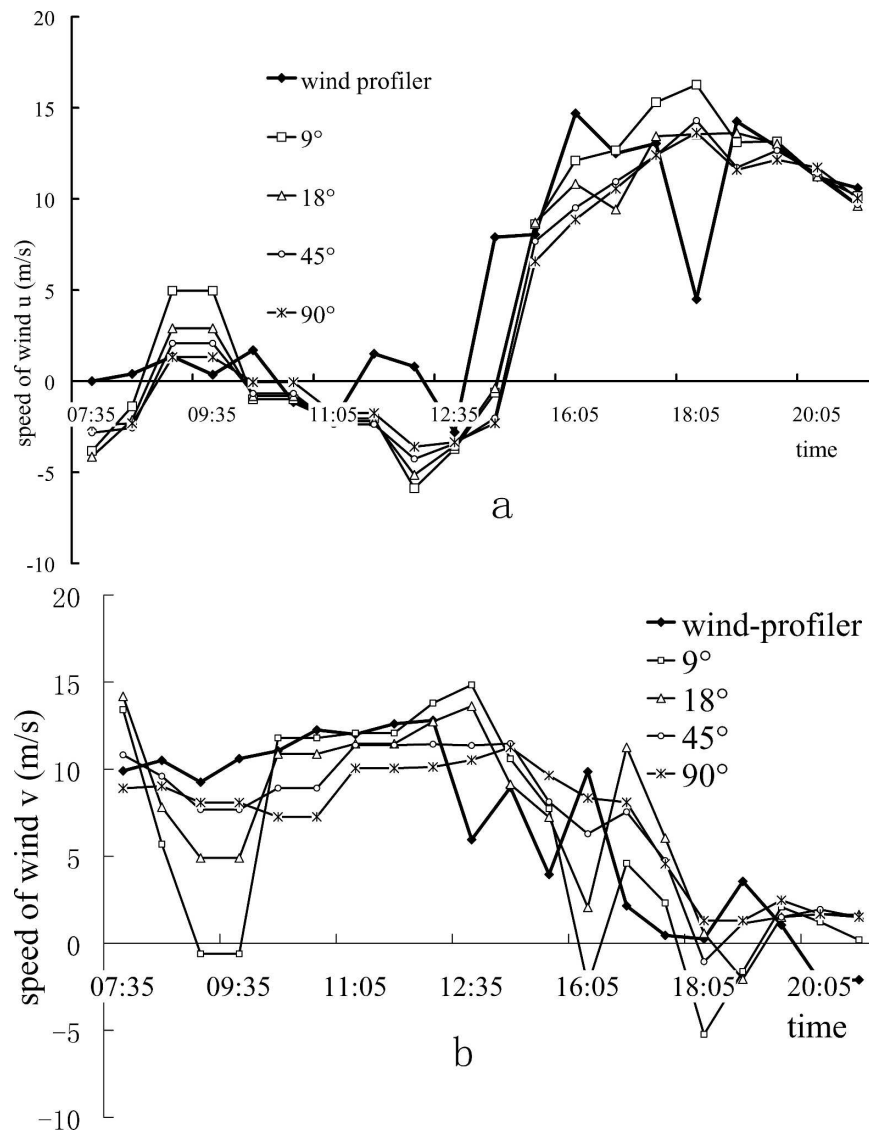


FIG. 3. Doppler-radar-retrieved and wind-profiler-observed (a) u and (b) v at QingPu from 0735 to 2035 UTC 5 Aug 2001. Unit: m s^{-1} .

90° , the correlation coefficients are not increased and the square mean errors are not decreased significantly. It also can be seen in Fig. 2 and Table 1 that in using a larger sector length, the retrieved wind is closer to the average value.

5. Conclusions and discussion

In this paper, it is shown that the commonly used approaches of the VAD, VAP, and UW method to retrieve wind fields from single-Doppler winds are special cases of a general relationship. Based on that relationship, an integrating VAP (IVAP) method is developed that uses the Doppler winds and their variation

within an azimuth sector to retrieve wind fields instead of only two neighboring points. Because of the short-wave filtering property of the IVAP method, a short-wave filter is not as necessary as in the VAP and UW methods. Given a larger sector length, a higher precision with lower horizontal resolution wind field can be obtained while a smaller sector length gives a lower precision and higher resolution. The IVAP method allows a choice of the sector length to get a wind field with a required precision or horizontal resolution, which are shown in a case study.

The comparison of wind-profiler data to IVAP method retrieved winds shows that the IVAP method gives a very good wind estimate. However, the ratio-

TABLE 2. Correlation coefficients and square mean errors between wind-profiler-observed and IVAP retrieved winds.

Sector length	<i>u</i>		<i>v</i>	
	Correlation coef	Square mean error	Correlation coef	Square mean error
9°	0.844	2.29	0.401	3.61
18°	0.873	1.99	0.475	2.92
45°	0.852	2.09	0.650	2.29
90°	0.852	2.04	0.625	2.30

nality and possibility in practical application of this method should be examined carefully in the future using plentiful data such as dual-Doppler data.

Acknowledgments. I wish to express my appreciation to Professor Zuyu Tao (Peking University) who provided valuable discussion that has given me encouragement in this study, and Qian Xing (Shanghai Meteorological Center, CAAC) who provided the Doppler radar data. Comments from the reviewers led to improvements in the content of the paper and are gratefully acknowledged. This research was sponsored by the National Natural Science Foundation of China Grant 40405012 and the Ministry of Science and Technology of China Grant 2005DIB3J104.

REFERENCES

- Browning, K. A., and R. Wexler, 1968: The determination of kinematic properties of a wind field using Doppler radar. *J. Appl. Meteor.*, **7**, 105–113.
- Caya, D., and I. Zawadzki, 1992: VAD analysis of nonlinear wind fields. *J. Atmos. Oceanic Technol.*, **9**, 575–587.
- Fu, G., Y. Duan, X. Liang, and S.-P. Xie, 2004: Observations of a heavy rainfall event in Shanghai on 5 August 2001. *J. Meteor. Soc. Japan*, **82**, 1793–1803.
- Kapitza, H., 1991: Numerical experiments with the adjoint of a nonhydrostatic mesoscale model. *Mon. Wea. Rev.*, **119**, 2993–3011.
- Persson, P., and T. Andersson, 1987: A real-time system for automatic single-Doppler wind field analysis. *Proc. Symp. on Mesoscale Analysis and Forecasting*, Vancouver, BC, Canada, ESA, ESA Publication SP-282, 61–66.
- Qiu, C.-J., and Q. Xu, 1992: A simple adjoint method of wind analysis for single-Doppler data. *J. Atmos. Oceanic Technol.*, **9**, 588–598.
- Rinehart, R. E., 1979: Internal storm motions from a single non-Doppler weather radar. Tech. Note NCAR/TN-146+STR, 262 pp.
- Shapiro, A., P. Robinson, J. Wurman, and J. Gao, 2003: Single-Doppler velocity retrieval with rapid-scan radar data. *J. Atmos. Oceanic Technol.*, **20**, 1758–1775.
- Sun, J., D. W. Flicker, and D. K. Lilly, 1991: Recovery of three-dimensional wind and temperature fields from simulated Doppler radar data. *J. Atmos. Sci.*, **48**, 876–890.
- Tao, Z., 1992: The VAP method to retrieve the wind vector field based on single-Doppler velocity field (in Chinese). *Acta Meteor. Sin.*, **50**, 81–90.
- Tuttle, J. D., and G. B. Foote, 1990: Determination of the boundary layer airflow from a single Doppler radar. *J. Atmos. Oceanic Technol.*, **7**, 218–232.
- Waldteufel, P., and H. Corbin, 1979: On the analysis of single-Doppler radar data. *J. Appl. Meteor.*, **18**, 532–542.
- Xu, Q., C.-J. Qiu, and J.-X. Yu, 1994a: Adjoint-method retrievals of low-altitude wind fields from single-Doppler reflectivity measured during Phoenix II. *J. Atmos. Oceanic Technol.*, **11**, 275–288.
- , —, and —, 1994b: Adjoint-method retrievals of low-altitude wind fields from single-Doppler wind data. *J. Atmos. Oceanic Technol.*, **11**, 579–585.
- , —, H.-D. Gu, and J.-X. Yu, 1995: Simple adjoint retrievals of microburst winds from single-Doppler radar data. *Mon. Wea. Rev.*, **123**, 1822–1833.
- Zawadzki, I. I., 1973: Statistical properties of precipitation patterns. *J. Appl. Meteor.*, **12**, 459–472.